Chapter 6

Spots size

6.1 Foreword

In Chapter 3, I discussed the general morphology of the Io footprint, without considering the size of the different features in detail. We will now focus on this particular question and, once again, we will see that "simple" measurements of IFP characteristics on FUV images indeed provide us with precious information on the ongoing physics. The reader might be surprised that the essential but controversial problem of the IFP spots size appears so late in the present manuscript. This delay is totally deliberate. In Chapters 4 and 5, crucial Io footprint characteristics have been analyzed and new measurement techniques have been developed, which will prove to be indispensable to accurately establish the spatial extent of the IFP spots. The new IFP reference oval provides a great help in automating the measurement procedures, since we now know where to expect the spots to appear. Additionally, our systematic analysis of the relative positions of the spots showed that these features have to be interpreted individually. The study of the tail vertical extent led to the development of a new technique to systematize the analysis of emissions appearing above the limb. This method will now be extended to determine the spots altitude and vertical extent.

Therefore, the present chapter stands in the continuity of our previous investigations of the Io footprint characteristics. This present question is: How large is the Io footprint? This quantity is supposed to give us information on the size of the interaction region at Io. However, by looking for the answer to this obvious question, we will also find potentially surprising clues ... on the Jovian magnetic field.

6.2 Introduction

Various and potentially contradictory numbers can be found in the literature concerning the spatial extent of the Io footprint. *Connerney et al.* (1993) depicted the infrared IFP as a point source which could be 5° long at maximum. They suggested that the observed extension could be longer than the instantaneous charged particles precipitation area because the lifetime of H_3^+ lies between 10 and 1000 s. On one hand, studies based on the Faint Object Camera (FOC) onboard HST (*Prangé et al.*, 1996; *Prangé et al.*, 1998) describe the spot as being 400 (-200,+100) km long. Similarly, *Vasavada et al.* (1999), described the Io footprint as a 450 ± 100 km diameter circular patch, based on visible images acquired with the SSI instrument on board the Galileo probe. These results lead to the conclusion that the IFP size roughly corresponds to the projected size of Io in the Jovian ionosphere (see Figure 6.5 for more details). On the other hand, *Clarke et al.* (1996), using the second generation Wide Field and Planetary Camera 2 (WFPC2), measured the Io footprint spot to be as long as 1000 to 2000 km, much larger than Io's projected diameter. Later studies making use of the third generation Space Telescope Imaging Spectrograph (STIS) instrument showed that the Io spot can even be as long as 20° longitude (*Clarke et al.*, 2002). The authors explained the discrepancy with the FOC based measurements by the lack of sensitivity of this instrument, which would only be able to detect the brightest part of the emission. *Clarke et al.* (2002) found that the FUV emissions related to Io could sometimes appear as a pair of spots instead of a single one. These spots were found to be 12° apart at maximum and these authors noted that this length roughly corresponds to the mapping of the size of the stagnant plasma wake at Io (*Hinson et al.*, 1998). Consequently, they interpreted the brightest part of the Io footprint, no matter it is formed by one large spot or by multiple spots, as the signature of an interaction region consisting of Io and its plasma wake. On the contrary,*Gérard et al.* (2006) considered the different spots as distinct features and studied the spots multiplicity on a wider range of STIS images. By isolating the main spot, they measured its typical length to be on the order of 0.9° longitude. *Serio and Clarke* (2008) also measured the Io footprint size, but in a quite different way. They measured the footprint diameter as the FWHM width of the footprint perpendicular to the contour direction. They found that this quantity ranges from 500 to 2000 km and that it is not correlated with the Io centrifugal latitude (Figure 6.1). Finally, *Gladstone et al.* (2007) measured the main spot width

to be 400 km large. They also found that the the vertical extent of the main spot appears as long as 1000 km.

From the above review of the different numbers for the Io footprint size, it appears that the same name is sometimes used for different concepts. The Io footprint main spot is an emission volume which has a length (along the contour), a vertical extent and a width (perpendicular to the contour direction and horizontal). Depending on the orientation of the spot on the image, the measurable "size" of the footprint is usually a combined projection of these three parameters, with the exception of some particular cases. This situation was taken into account by *Prangé et al.* (1996), who clearly made the difference between the measured width and length. Since the exposure time may lead to strong corotational blurring, they rather relied on the width measurement, made possible by the particular location of the spot close to the limb. Then they verified that the measured length would be compatible with a 400 km spot blurred by the motion of the spot during the exposure. Nevertheless this noting does not necessarily invalidate issues related to the poor quality of FOC images. On the other hand, the footprint radii from *Serio and Clarke* (2008) appear to be a mix of projected width and vertical extension; a mix which is strongly dependent on the position of the spot on the image.

In order to determine the shape and size of the different spots, we made use of subsets of images showing the spots from different points of view. When the spots lie close to the central meridian line the footprint is generally seen from the side: a favorable configuration to estimate the lengths along the contour. On the other hand, some particular IFP curtain configurations observed when the spots are close to the limb show the IFP from above, allowing us to measure its width. Finally, we showed that it is possible to measure the vertical extent of the tail emissions since we can detect the point where the tail is right above the limb plane. Unfortunately, no image has been acquired in a configuration such that the spots are exactly above the limb, but there is a way to circumvent this issue.

6.3 The spots length

In the introductory section of this chapter, we have seen that the footprint length, whatever it means, has been expressed both in degrees of longitude and in kilometers. Which way is the more meaningful? How do we convert one unit into the other? Surprisingly, these questions do not have trivial answers. At first sight, units of

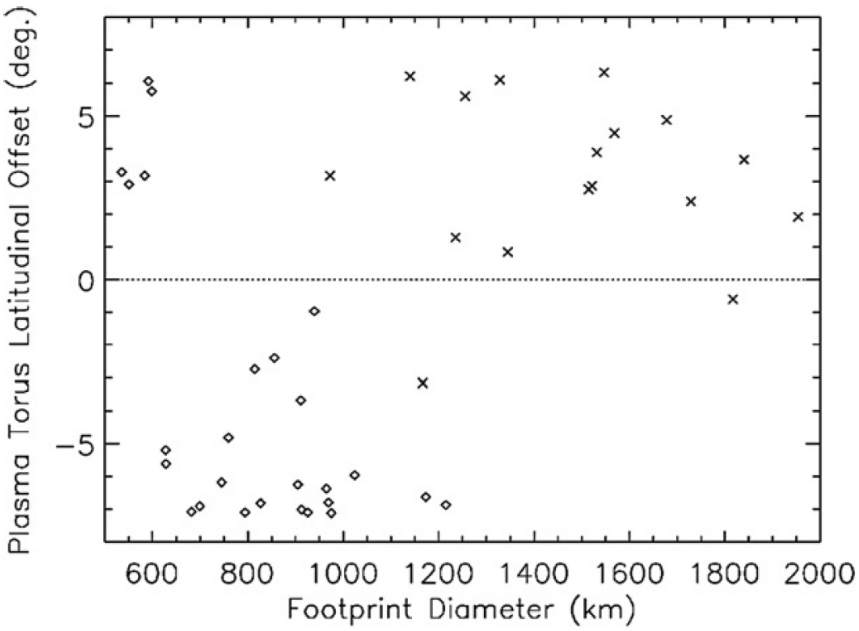

Figure 6.1: Plot of the footprint diameter as a function of the position of Io in the plasma torus. This quantity is measured as the FWHM of the emission perpendicularly to the contour direction. The diamonds correspond to the North and crosses to the South. (from *Serio and Clarke* (2008))

degrees seem far more convenient since they seem to allow an easy comparison with characteristic quantities in the Io orbital plane. However, this projection would only be accurate if the Jovian magnetic field was a perfect dipole aligned with the Jovian rotation axis. Actually, one degree of longitude measured at one point along the contour could correspond to a very different distance in kilometers than at another point, because of the off-centered configuration of the footpath, especially in the North. Additionally to this effect, the conversion from ionospheric longitudes to Io orbital plane longitudes is complicated by the convergence/divergence of the field lines[1] related to magnetic field anomalies. One definitive way to deal with the problem would be to map the distances along the magnetic field lines as we did on Figure 3.4. However, even if the results seem convincing at first sight, the accurate measurement of the footprint positions shed some doubts on the ability of the current magnetic field models to perform reliable mappings (Chapter 4).

Consequently, the question related to the link between degrees and kilometers remains, but the new Io reference oval can help us. Figure 6.2 shows the variation of the number of kilometers per degree measured in the Io orbital plane (solid line) as a function of the Io System III longitude based on our new reference contour. Therefore, for a given Io longitude the plot indicates the number of kilometers covered by the footprint when Io covers one degree along its orbit. The mean value is 481 km/° in the North and 463 km/° in the South. It is noteworthy that this quantity is fairly constant in the South but has two large peaks in the North, one at ∼50° and another one at ∼280°. These peaks mean that the spot moves quickly in these places, which can be explained by a divergence of field lines. The large increase around 50° of Io System III longitudes corresponds to IFP longitudes around 100°. Consequently, this IFP acceleration area clearly matches to the anomaly region described in *Grodent et al.* (2008a). Where does the second peak come from? A possible answer is that this peak corresponds to the so called "Dessler anomaly" (*Clarke et al.*, 2004). Indeed, the acceleration of the footprint along the contour suggests a divergence of the magnetic field lines in the contour direction. If this divergence (relative to the dipolar configuration) takes place in every direction, this could indicate that the magnetic field intensity is lower in this area, which could correspond to an "active sector" for radio emissions. We should however note that this argument is not a proof, since there is no one-to-one correspondence between a

[1] Two nearby field lines intercepting Io's orbit are always expected to converge when approaching the planet. By "diverging", I mean that they converge less than expected for a dipolar field.

divergence along a particular direction and the decrease of the field strength. In the southern hemisphere the VIP4 model predicts that the field intensity along the Io contour could vary by a factor of ∼2 without giving rise to any footprint acceleration, in accordance with the observations.

Nevertheless, our goal is to allow comparisons between distances measured in degrees and distances measured in kilometers. Therefore, we are interested in the number of kilometers per degree as measured on Jupiter. This quantity is represented by dashed lines on Figure 6.2. The mean values are 625 km/° in the North and 497 km/° in the South. However, we note that the conversion coefficient can vary by a factor of ∼5 in the North and ∼2 in the South. Consequently, there is no unique coefficient to convert degrees to kilometers. We will thus use both units to measure the MAW spot length before discussing which is the more convenient unit.

The first step consists in selecting images where the MAW spots are less than 30 degrees away from the central meridian line. We automatically extracted stripes along the IFP reference oval described in Chapter 4. Each stripe begins 5000 km upstream of the expected MAW spot position. Then, every 25 km in the downstream direction, we locate the corresponding pixel on the image and report its brightness. We repeat this operation for altitudes ranging from 0 to 2000 km. Once the stripes are formed, we add the brightnesses vertically in order to generate brightness profiles. The profiles are considerably more extended in the downstream direction because the tail emissions add to the downstream spots. Consequently, measurements of the profiles full width at half maximum (FWHM) cannot be used directly since they are usually contaminated with emissions unrelated to the MAW spot. Therefore, we chose to measure the upstream half width at half maximum (HWHM) in order to characterize the length of the main spot as if it were isolated from the other IFP emissions. The actual FWHM is then assumed to be twice as large as the measured HWHM. Figure 6.3 presents the main spot length FWHM expressed both in degrees and in kilometers. We note that the results in degrees are relatively constant for all longitudes and both hemispheres. The mean value is ∼900 km. Northern hemisphere measurements are only available between 110° and 230° System III longitudes. Based on Figure 6.2, we note that our value is in accordance with the 0.9° measured from *Gérard et al.* (2006). On the other hand, the mean FWHM expressed in degrees of longitude on the planet is twice longer in the South than in the North. Additionally, the southern hemisphere length varies with the Io longitude in an anti-correlated way compared to the number of kilometers per degree, as expected from previous

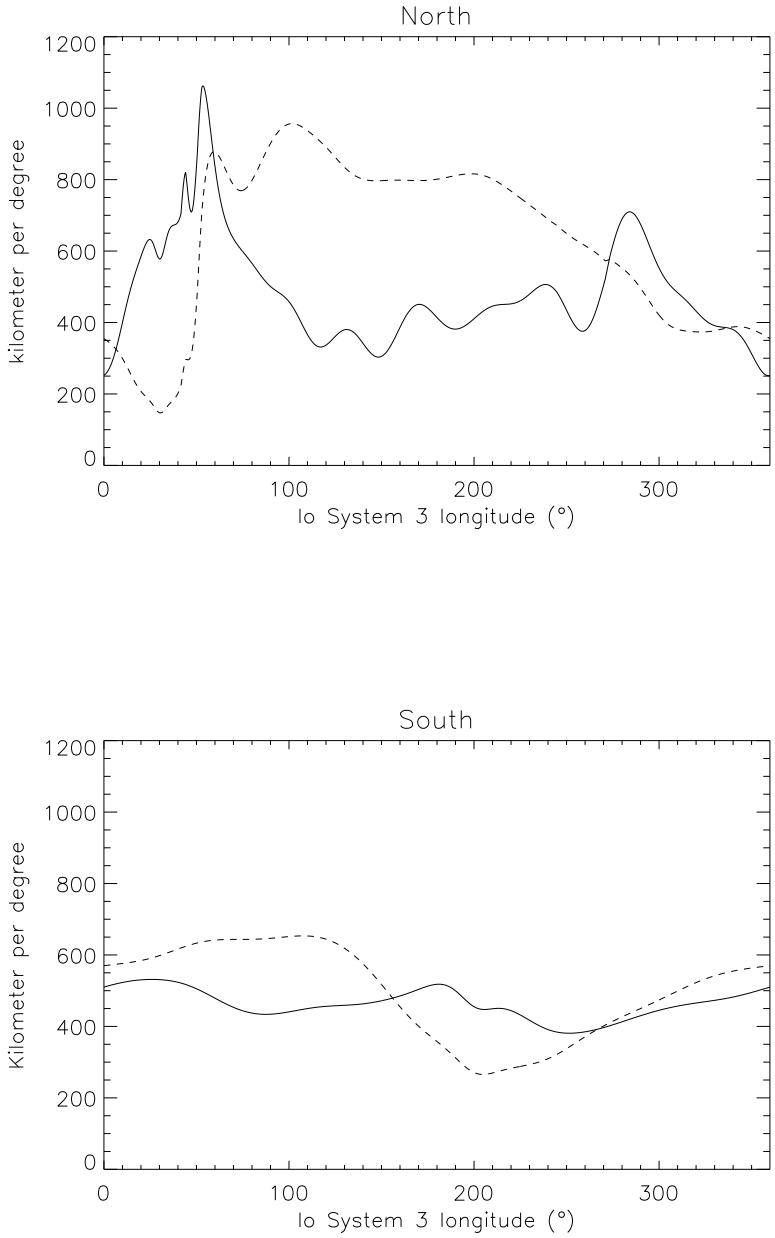

Figure 6.2: Evolution of the number of kilometers per longitude degree as a function of the System III longitude of Io for the northern and southern hemispheres. The solid line corresponds to longitudes measured along the orbit of Io while the dashed line corresponds to longitudes measured on the planet.

considerations.

The fact that both reference contours have roughly the same size and that the main spot length does not vary much (outside the anomaly regions) indicate that, compared to the dipole case often assumed in theoretical models, the observed contours are off-centered and distorted but the length measured in kilometers does not vary significantly. As a consequence, these distances should be preferentially used when comparing Io footprint characteristics.

In figure 6.3, three STIS southern hemisphere data points have considerably higher values than the other data points. These points are not outliers but correspond to exceptionally long footprints like the one shown in Figure 3.6 a. The plots clearly demonstrate that these cases are atypical and should be considered with caution when drawing conclusions on the spots length.

We have seen that the Io footprint typical length was around 900 km. This observationally derived value should be compared to two quantities: the length covered by the MAW spot on the image during a typical exposure time and the projected Io diameter along magnetic field lines. Figures 6.4 displays the length covered by the IFP in a reference frame fixed in local time for a typical 100 seconds exposure time. This quantity approximately varies in a similar way as the above mentioned number of kilometers per degree in the Io orbital plane. The main difference is that the distances are now computed in local time reference frame and not in a System III reference frame. This means that they combine not only the motion of the footprint along the contour, but also the apparent motion of the contour as seen from the Earth. The values plotted here should be projected relatively to the image viewing angle to provide the actual IFP motion on the image. However, this later step is not necessary for the issue we would like to discuss here. The displacement of the IFP during the exposure time generates a motion blur and we would like to know how this affects the measured footprint length. In the southern hemisphere, the covered distance ranges from $\sim$ 200 km to $\sim$ 350 km, while in the North, the distance varies from $\sim$50 km to $\sim$ 800 km. If we model the MAW spot brightness profile with a Gaussian function and if we convolve it with a step function as long as the original Gaussian FWHM, the resulting FWHM is only 20% longer. We will see in Chapter 7 that the footprint spots can experience brightness variations on the order of 50% of the intensity on timescales of one minute. In the worse case scenario, the spot brightness first decreases by a factor of 2 until the middle of the exposure time and then increases again up to the maximum. In this case, the length increases by

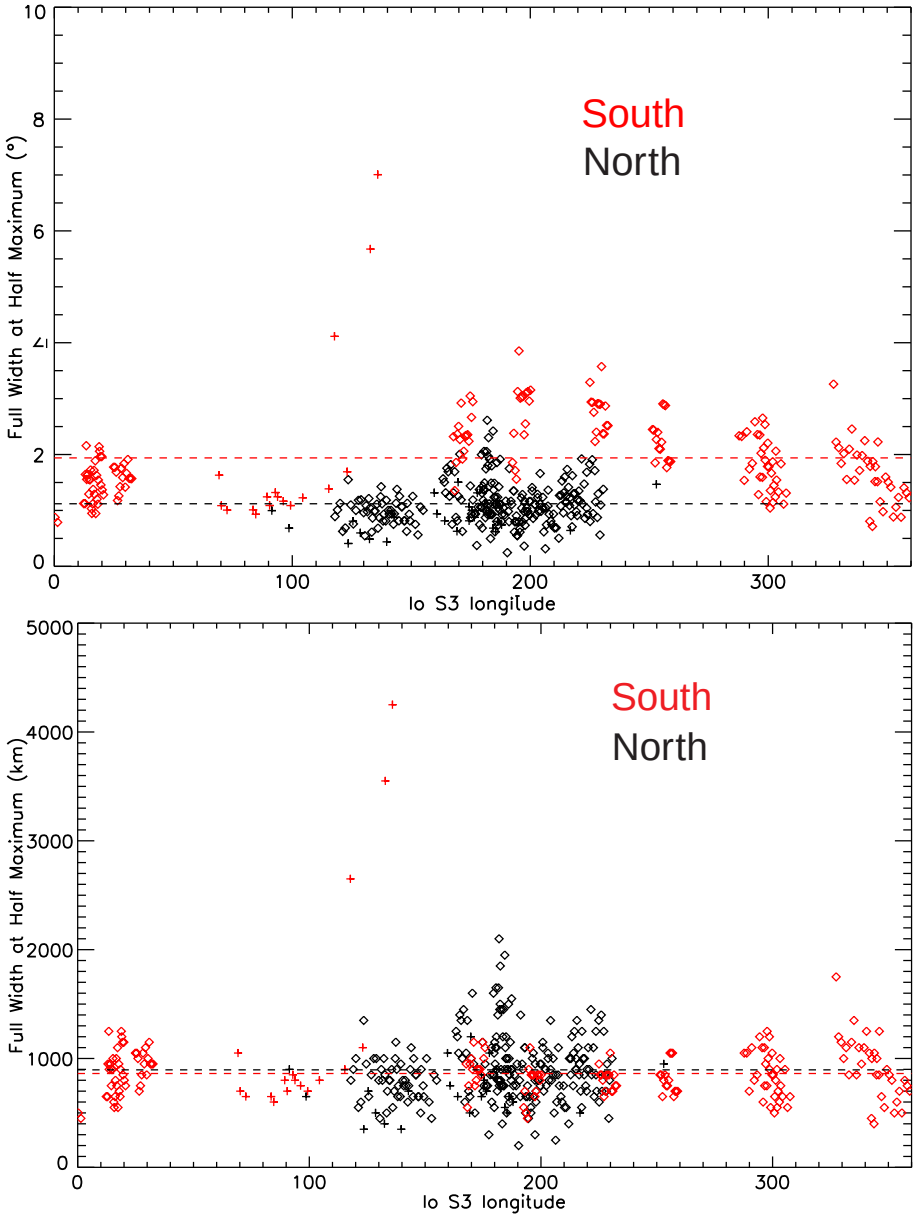

Figure 6.3: Length of the Io footprint main spot as a function of the Io System III longitude. The data points corresponding to STIS measurement are represented with crosses while ACS data are noted with diamonds. Black symbols are for measurements in the northern hemisphere while red symbols are measurements in the southern hemisphere. The Full Width at Half Maximum represented in the plots is actually computed as twice the Half Width at Half Maximum.

approximately 30%. Thus, even in the most critical cases, the length measured on 100s exposure images is only moderately affected by the motion blurring. However, in this study no measurements have been made in these critical areas of the northern hemisphere where the MAW spot length is difficult to observe. If the covered distance is one half of the initial Gaussian FWHM, the length increases by 7% at maximum. Consequently, we can consider that the measured length corresponds to the instantaneous length.

Figure 6.5 shows the size of the unperturbed Io flux tube footprint in the northern hemisphere according to the VIP4 magnetic field model. The IFT length varies from $\sim$ 200 km to $\sim$ 350 km. The FWHM of the STIS and ACS point spread functions are barely larger than two and one pixels respectively and, accordingly, the widening of the spot cannot be attributed to instrumental effects. As a result, the MAW spot length shown on Figure 6.3 appears to be three to four times more elongated than the expected flux tube length. This result does not necessarily mean that the interaction region at Io is three to four times as large as Io. The plasma interaction between Io and the Jovian magnetosphere implies a piling up of the field lines at Io. Therefore, it is expected that the real (i.e. perturbed) flux tube length is larger than the unperturbed one. However, the spot is not located at the foot of the Io flux tube but rather at the foot of the current carrying Alfvén wing. *Jacobsen et al.* (2007) showed that non-linear effects on the Alfvén waves propagation could considerably increase the length of the Alfvén wing (Figure 6.6). Additionally, *Jacobsen et al.* (submitted) showed that such non-linear effects are necessary to explain why the electron beams observed by Galileo are located so close to Io.

6.4 The spots vertical extent

In the previous chapter, we made use of images where the tail emissions were observed above the Jovian limb. Here we consider a subset of these images where the main spot can be seen above the limb. Contrary to the tail, we cannot be sure that the main spot is in the limb plane, or, more exactly, we are sure that the spot in not in the limb plane. Consequently, the apparent altitude is not the real altitude and we have to find another strategy to estimate the actual altitude of the main spot emission. Since we know the longitude and the latitude of the main spot thanks to the new reference contour, we can compute the expected MAW position on the image if its real peak altitude is the same as for the tail (i.e. $\sim$ 900 km). If the

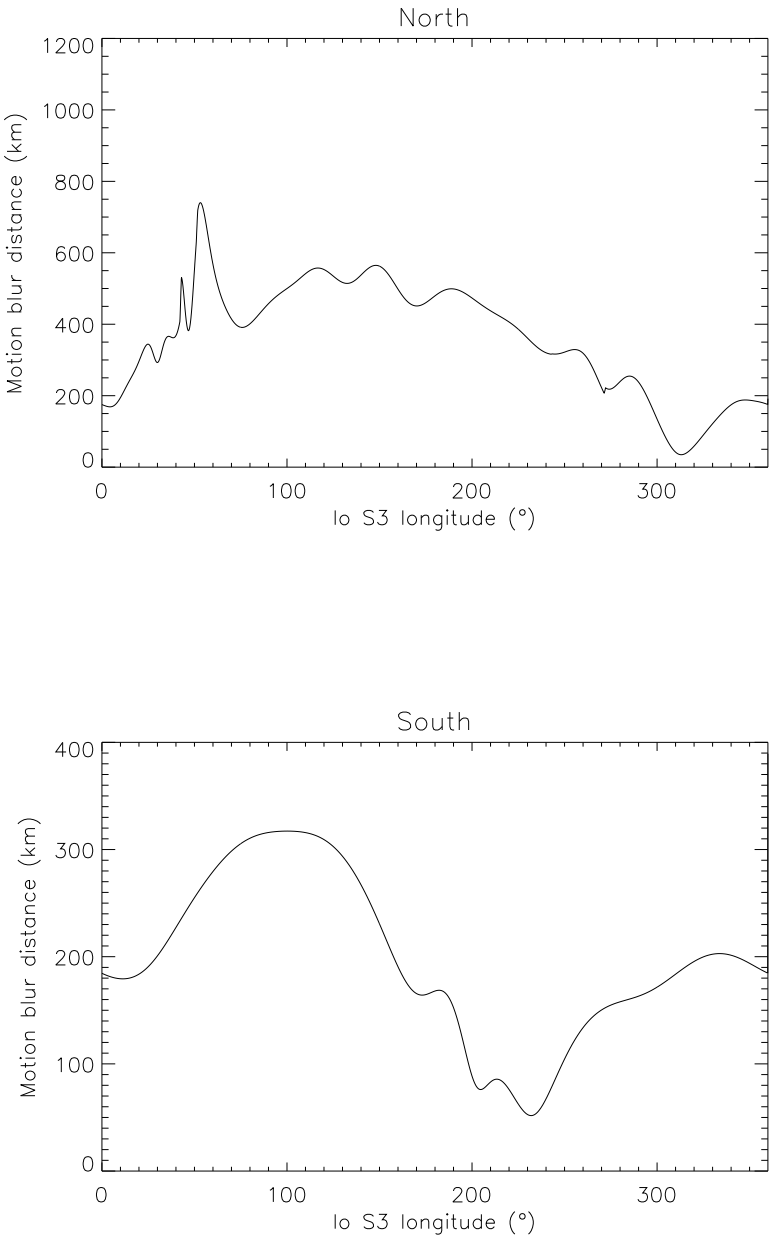

Figure 6.4: Plots of the motion blur distance for an exposure time of 100 seconds as a function of the Io System III longitude. The motion blur distance is the distance covered by the MAW spot in a reference frame fixed in local time. Contrary to Figure 6.2, this quantity includes both the motion of the footprint along the contour and the motion of the contour owing to the planetary rotation.

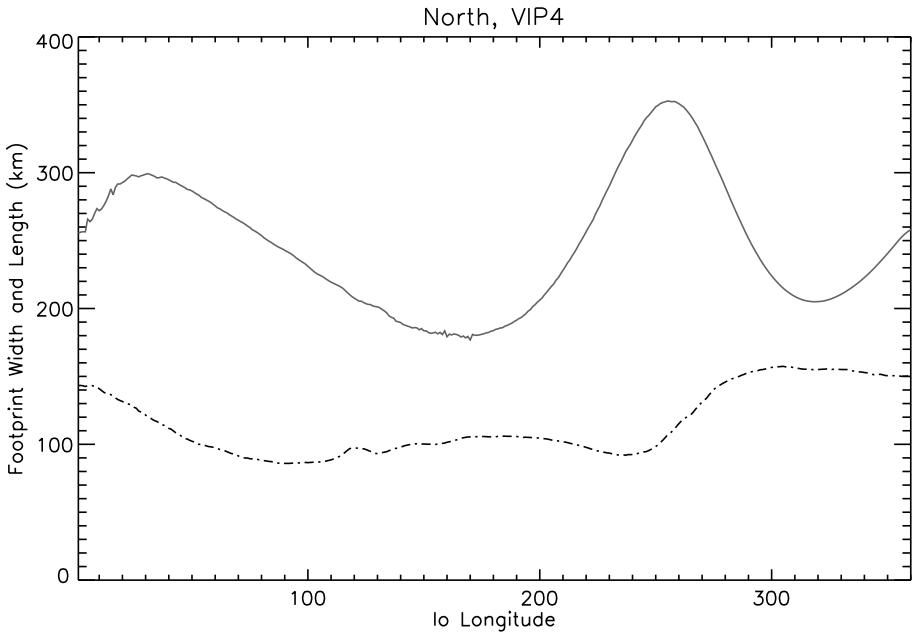

Figure 6.5: Projected size of Io along unperturbed magnetic field lines as modeled by VIP4 for the northern hemisphere. The solid line represents the Io diameter along the Io orbit projected in the northern Jovian ionosphere. This quantity thus stands for the length of the Io flux tube (IFT) footprint. The dashed line represents the diameter of Io along the Io-Jupiter line projected in the northern Jovian ionosphere. This quantity thus stands for the width of the Io flux tube (IFT) footprint.

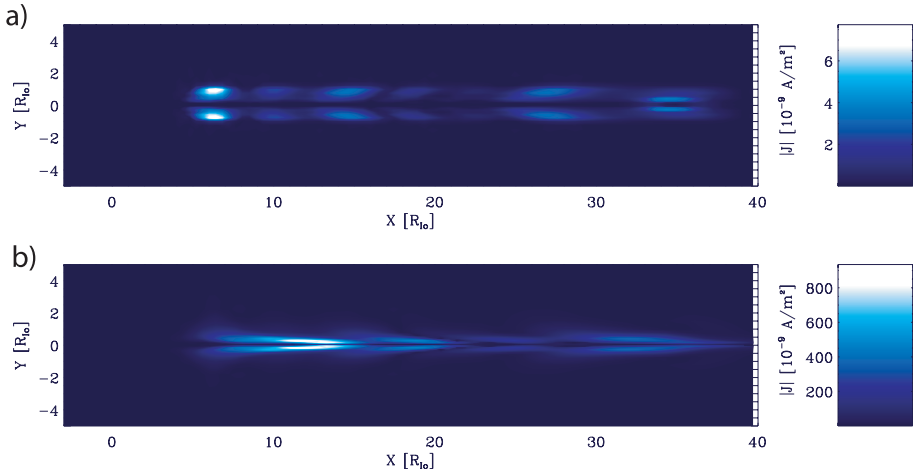

Figure 6.6: Projection of the absolute value of the current density in the northern Jovian ionosphere in the case of a quasi-linear interaction (a) and of a strongly non-linear interaction (b). The non-linear effects considerably stretch the Alfvén wing in the corotation direction, which could explain why the observed length of the MAW spot corresponds to three to four times the length of the unperturbed Io flux tube. (from *Jacobsen et al.* (2007))

observed peak altitude differs significantly from the simulation, this would indicate that the main spot is not at the assumed altitude.

During the 10862 observation program, the IFP MAW spot appears above the planetary limb for 14 orbits. Similarly to *Bonfond et al.* (2009), we gather image data as sets of 3 successive images and perform radial scans on the Io footprint area. This time, we are not looking for the highest peak altitude as a function of the scan angle, but we seek the maximum brightness. We compare the peak altitude of this particular profile with the simulated peak altitude (Figure 6.7). The mean difference between the modeled altitude and the observed one is 85 km with a standard deviation of 155 km. We can thus reasonably conclude that the the MAW spot peak altitude is similar to the tail peak altitude, which confirms results from color ratio measurements (see *Gérard et al.* (2002) and Chapter 5).

An important result from Chapter 5 is that the vertical scale height of the tail emission is so large that its width can be modeled only by assuming a kappa energy distribution for the incoming electrons. This result is not in agreement with expectations from electron acceleration by a static electric potential and favors mechanisms related to inertial Alfvén waves (*Swift*, 2007). Consequently, the shape of the emission vertical profile of the MAW spot is also expected to provide us with information

on the acceleration mechanism. Fits of a Chapman profile (Equation 5.1) on the observed curve indicates that the mean scale height is 366 km ± 53 km. These values are similar to those observed for the tail. Additionally, a Chapman profile with such a scale height has a FWHM of ∼850 km, which is consistent with the estimates from *Gladstone et al.* (2007). As a conclusion, the precipitating electrons generating the IFP main spot appear to have the same characteristics as for the tail, i.e. a kappa energy distribution with a mean energy $\sim 1-2$ keV.

On one single orbit, leading spot emissions can also be observed above the limb. The brightness and peak altitude profiles as a function of the rotation scan angle[2] are shown on Figure 6.7. While the observed and the modeled altitudes are fairly similar in the tail and for MAW spot, the observed altitude appears to be $\sim$ 200 km smaller. The fact that the TEB emissions peak at a lower altitude could also explain some misalignment between the TEB spot and the remainder of the tail. An example of such a misalignment can be seen on the top South stripe of Figure 1.10. This slight shift could be interpreted as a latitudinal shift or an altitude shift. Our new observations clearly favor the latter. These lower altitudes suggest that the TEB spot electrons mean energy is larger than for the MAW spot and the tail.

6.5 The spot width

The actual Io footprint width can be estimated only if two restricting conditions are fulfilled. First, the viewing angle should be such that the main spot is seen from the front or from above. Second, the exposure time should be short enough to avoid significant shift of the IFP position during the exposure. This latter constraint imposes the use of images derived from time-tag sequences.

Similarly to the method applied to estimate the spots length and vertical extent, the first step consists in identifying the images where the footprint is in such a configuration that the main spots and the beginning of the tail are seen from the front or from the top. Unfortunately, the number of suitable time-tag sequences is limited to two. In order to avoid the motion blur which affects the width without losing too much signal, the time-tag sequence list has been divided into 10-second exposure time images. These images were subsequently shifted in order to compensate for the

[2]Our method consist is taking radial cuts while rotating the planet on the images. 0° corresponds to the equator and -90° corresponds to the South pole, but the intermediate values are not strictly equivalent to latitudes because of the inclination of the planet.

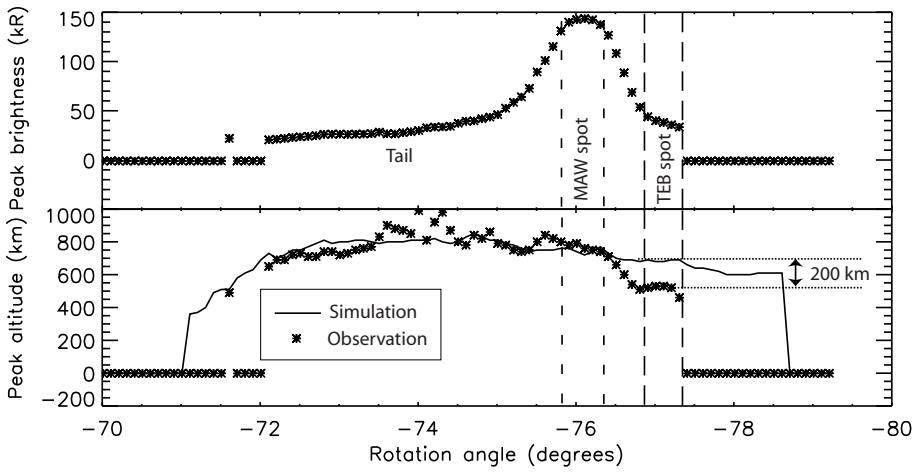

Figure 6.7: Example of tails and spot profiles above the limb as a function of the rotation scan angle (stars). The expected apparent altitude of an Io contour located at 900 km is represented in solid line. The MAW spot corresponds to the peak in the brightness profile. All along the tail as well as in the MAW spot region, the observed and the predicted apparent peak altitudes match fairly well. In this example, a faint TEB emission also appears upstream of the MAW. Its apparent altitude is 200 km lower than expected.

IFP motion.

Figure 6.8 shows an example of images generated from the same sequence with and without the motion compensation. It is noticeable that the motion seems to increase the IFP width, which directly indicates that the instantaneous IFP curtain width is significantly smaller than the motion blur extent. The width is measured by extracting a brightness profile perpendicular to the contour. However, the width of this profile is very dependent on the orientation of the footprint on the image, and thus does not represent the actual curtain width. Actually, even in our very restrictive case selection, the footprint is never observed exactly from the front or exactly along magnetic field lines and thus we have to model the real image geometry to take these orientation effects into account. To demonstrate the existence of these effects and evaluate their impact, we made use of the 3D IFP emission model we will use in the next chapter in order to simulate the apparent IFP width with different actual input width. The model will be described extensively later, but for now, it suffices to note that it consists in simulating the FUV optically thin emissions for an IFP formed of three independent spots and an extended tail. The length and the vertical extent of these different features is set according to the measurements

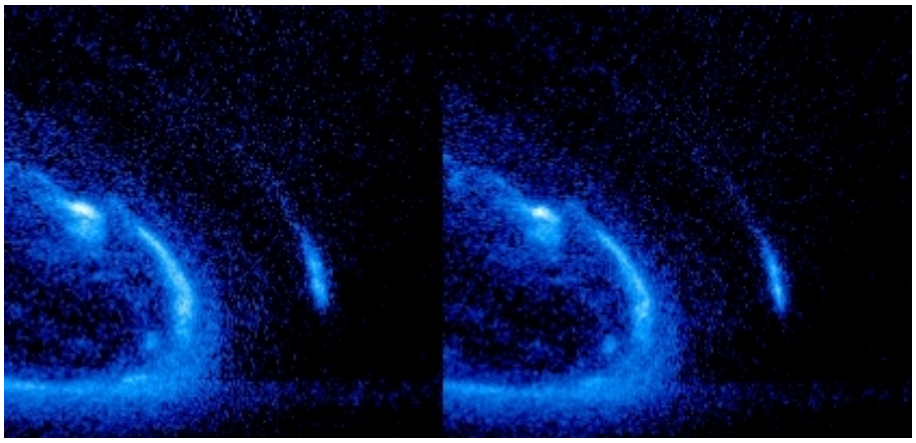

Figure 6.8: Example of Io footprint as seen from above without (left) and with motion compensation (right).

described above. We generate images of the IFP in agreement with the actual IFP geometry but varying the width. Among the unavoidable hypotheses we have to take on the IFP geometry (see section 7.4 for more details), we postulate that all the IFP features, i.e. the three spots under consideration and the tail, have the same width. Then we compare these modeled apparent widths with the measured one (Figure 6.9).

In both cases, the observed profile is as thin or even slightly thinner than the thinnest model profile. We note that, because of the finite pixel size and PSF size, at some point, reducing the input width has a minor impact on the model output. As long as the simulated FWHM input remains less than ∼170-190 km, the modeled width remains fairly similar to the measured ones. Major differences only arise when this threshold is overtaken. As a result, only an upper limit can be estimated for the IFP width and its value is around 200 km.

The expected projection of Io's width along VIP4 magnetic field lines lies between 100 and 160 km (Figure 6.5). Contrary to the spots length, no interaction model predicts a significant increase of the IFP width compared to the projected Io width (Figure 6.6). Our measurements only provide a maximum value for the width, but they show that the diameter of the interaction region as seen from the front cannot be wider than twice the size of Io. These values are in accordance with the idea that the IFP width is similar to the projected diameter of Io.

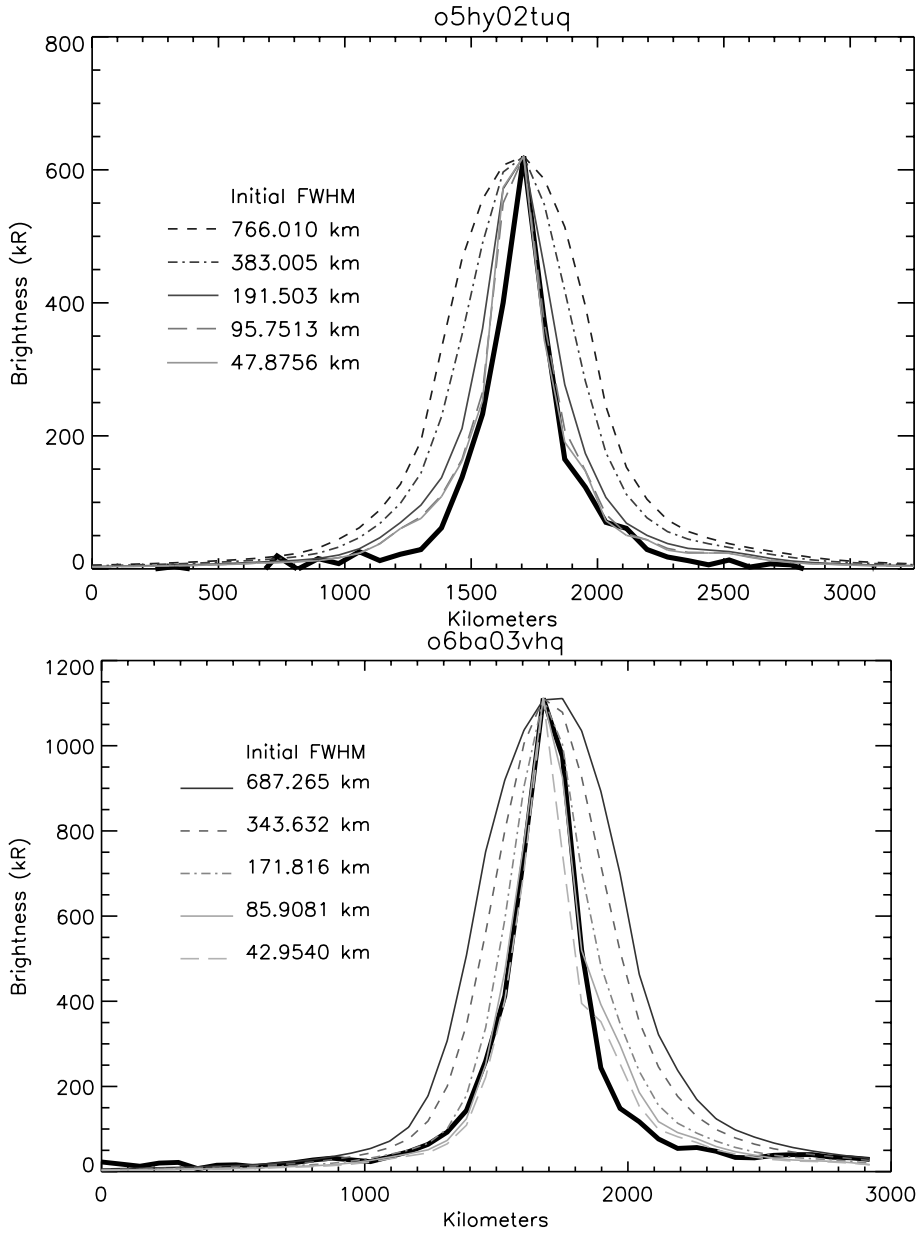

Figure 6.9: Comparison of measured Io footprint width profile with simulated output profiles computed with different input widths. Both cases are from the northern hemisphere. The Io System III longitude is 209° in the first case and 145° in the second one.

6.6 Conclusions

The size of the Io footprint is an important issue for understanding the Io-Jupiter interaction. Based on the apparent restricted size of the Io footprint on some images, some authors suggested that the interaction should be limited to Io itself. On the other hand, its apparent extended length as seen on other images led other authors to reach the opposite conclusion: i.e. the interaction region should be as large as the stagnating wake observed downstream of Io. We took advantage of the increased number of images benefiting from both high resolution and high sensitivity to sort out these contradictory results.

First of all, we argue that the 3D structure of the Io footprint has often been misunderstood. Following *Gérard et al.* (2006) as well as conclusions from the previous chapters, the different spots are distinct features that must be considered separately. Secondly, each feature has a length along the contour, a vertical extent and a width. Therefore, each image is a 2D projection of a three dimensional emission region. With the help of the observations catalog and our knowledge of the IFP spots location, we carefully selected subsets of images where the spots were respectively seen from the side, above the limb or from above.

The length of the main spot is on the order of 900 km FWHM. We showed that this value is not a consequence of the motion of the spot during the exposure nor caused by the instrumental PSF. This length is significantly larger than the size of Io but also significantly smaller than the size of the stagnating plasma wake when projected along unperturbed magnetic field lines. However, the field lines are indeed perturbed by the presence of Io and the subsequent broadening of the main spot length along the contour was expected from simulations, even if the core of the interaction remains relatively close to the satellite.

The IFP width measurement is by far the most delicate measurement. Our measurements only provide a maximum value ($\sim$ 200 km) but this number is also consistent with an interaction region restricted to the immediate Io neighborhood.

As far as the MAW spot vertical extent is concerned, no obvious difference is observed compared to the tail emissions. The peak altitude lies around 900 km and the scale height is approximately 350-400 km. As a result, the mean precipitating electron energy is on the order of 1-2 keV. Additionally, the broadness of the impinging electrons energy distribution suggests that inertial Alfvén waves are the root cause for the electrons acceleration. This conclusion is nevertheless less surprising for the

MAW spot than for the tail since no steady state was expected to be established for the spots. The TEB spot peak altitude appears to lie at 700 km, implying a larger mean electron energy than for the MAW spot.

As far as previous studies are concerned, we may conclude that the large spot sizes observed by *Clarke et al.* (2002) are untypical and 0.9-degree long MAW spots as measured by *Gérard et al.* (2006) correspond much more likely to the actual typical length. The small length of the IFP, as estimated from visible instruments (*Vasavada et al.*, 1999; *Gladstone et al.*, 2007) and from the FOC camera (*Prangé et al.*, 1996; *Prangé et al.*, 1998), is most probably a consequence of their limited sensitivity. Moreover, our observations confirm our initial expectation concerning the IFP diameter as measured by *Serio and Clarke* (2008): the quantity that they have measured is not the actual width of the IFP but the projection of its vertical extent, which is strongly dependent on the viewing angle.

Finally, our analysis of the motion of the MAW spot on the northern hemisphere shows the presence of two sectors where the spot is significantly accelerating along the contour. If these regions are associated with magnetic anomalies, the largest one is related to the large anomaly identified by *Grodent et al.* (2008a) while the smallest one could be related to the so-called "Dessler anomaly".